

# MICROSTRUCTURE/OXIDATION/MICROHARDNESS CORRELATIONS IN $\gamma$ -BASED AND $\tau$ -BASED Al-Ti-Cr ALLOYS

MICHAEL P. BRADY (NRC)\*, J.L. SMIALEK\*, AND D.L. HUMPHREY (NYMA, INC.)\*  
\*NASA Lewis Research Center, MS 106-1, Cleveland, OH 44135

## ABSTRACT

The relationships between alloy microstructure and air oxidation kinetics and alloy microstructure and microhardness in the Al-Ti-Cr system for exposures at 800°C and 1000°C were investigated. The relevant phases were identified as  $\tau$  ( $L1_2$ ),  $\gamma$  ( $L1_0$ ), r-Al<sub>2</sub>Ti, TiCrAl (laves), and Cr<sub>2</sub>Al. Protective alumina formation was associated with  $\tau$ , Al-rich TiCrAl, and  $\gamma$ /TiCrAl mixtures. Brittleness was associated with the TiCrAl phase and  $\tau$  decomposition to Al<sub>2</sub>Ti + Cr<sub>2</sub>Al. It was concluded that two-phase  $\gamma$  + TiCrAl alloys offer the greatest potential for oxidation resistance and room temperature ductility in the Al-Ti-Cr system.

## INTRODUCTION

Alloys in the Al-Ti-Cr system containing approximately 45-55 Al and 10-30 Cr (all compositions are reported in atom percent) were recently identified by Meier et al. as potential oxidation resistant coatings for  $\gamma$  +  $\alpha_2$  based titanium aluminides [1]. While such alloys are oxidation resistant, forming protective alumina scales at 800°C in air [2], they are also extremely brittle [1,3]. The goal of the present work was to co-optimize oxidation resistance and ductility in the Al-Ti-Cr system for use as a potential oxidation resistant coating alloy for  $\gamma$  +  $\alpha_2$  titanium aluminides.

## EXPERIMENTAL

Three alloys were selected to survey phase equilibria in the alumina-forming Al-Ti-Cr composition range identified by Meier et al. [2]: 45Al-40Ti-15Cr (alloy A), 55Al-30Ti-15Cr (alloy B), and 50Al-30Ti-20Cr (alloy C). Alloy A falls on the borderline for protective alumina formation, according to the Meier et al. oxidation map, and alloys B and C fall well within the protective alumina-forming composition range (Fig. 1). Based on the compositions measured for the phases observed in alloys A-C, 4 single-phase alloy compositions were also selected: 52Al-43Ti-5Cr ( $\gamma$  TiAl) and 37Al-34Ti-29Cr (TiCrAl) from alloy A, and 60Al-29Ti-11Cr ( $\tau$  cubic Al<sub>3</sub>Ti) and 42Al-31Ti-27Cr (TiCrAl) from alloys B and C (Fig. 1). All alloys were double arc-melted and cast into 13 X 13 X 50 mm rectangular cross-section buttons. No evidence of macro-segregation was observed, however all of the "single-phase" alloys were found to contain minor amounts of second phases [4,5].

The alloys were exposed for 100 h at 800°C or 1000°C in air. Microstructures were characterized by x-ray diffraction, wavelength dispersive electron microprobe analysis (pure element standards) and/or quantitative energy dispersive analysis ( $\tau$  phase standard), and scanning electron microscopy (SEM). Oxidation resistance was evaluated by box furnace weight gain screenings in room air and thermogravimetric analysis (TGA) in dry air. Alloy stability with alumina, a prerequisite for protective alumina scale formation, was examined by

Michael Brady

"sandwiching" an alumina fiber between 1 mm thick alloy blocks and hot pressing in vacuum at 1000°C for 2 h. Ductility trends were qualitatively evaluated by Vicker's microhardness (VHN). Further details are provided in refs. 4 and 5.

## RESULTS AND DISCUSSION

### Microstructure

The 1000°C phase equilibria determined from alloys A-C is shown in Fig. 1 [4]. Alloy A fell within a  $\gamma$  (TiAl) + TiCrAl laves (refer to ref. 6) two-phase field. This result is consistent with the microstructural data provided in ref. 7. Alloys B and C fell near the  $\tau$  ( $\text{Al}_3\text{Ti}+\text{Cr}$ )-TiCrAl edge of a  $\tau$ -TiCrAl- $\text{Cr}_2\text{Al}$  three phase field [4].

At 800°C, alloy A exhibited a  $\gamma$  + TiCrAl microstructure similar to that observed at 1000°C. However, after exposure at 800°C, the  $\tau$  phase in alloys B and C decomposed completely, within the detection limits of x-ray diffraction, to  $\text{Al}_2\text{Ti}$  and  $\text{Cr}_2\text{Al}$ . The decomposition of the  $\tau$  phase after exposure at 800°C was also observed in the "single-phase"  $\tau$  alloy, 60Al-29Ti-11Cr. Therefore, alloys B and C, which are representative of much of the alumina-forming Al-Ti-Cr composition range identified by Meier et al. (Fig. 1), are  $\tau$  + TiCrAl based at 1000°C and  $\text{Al}_2\text{Ti}/\text{Cr}_2\text{Al}$  + TiCrAl based at 800°C [4].

### Oxidation

The 100 h weight gains for the  $\tau$ , TiCrAl, and  $\gamma$  "single-phase" alloys after exposure at 1000°C or 800°C in room air are shown in Fig. 2. The  $\tau$  and Al-rich (42 Al) TiCrAl "single-phase" alloys exhibited protective alumina scale formation at both 1000°C and 800°C, although the TiCrAl alloy exhibited some transient Ti-based oxides at 800°C. The decomposition of the  $\tau$  phase to  $\text{Al}_2\text{Ti}$  and  $\text{Cr}_2\text{Al}$  at 800°C did not degrade oxidation resistance. Alloys B and C, the multiphase  $\tau$  ( $\text{Al}_2\text{Ti}$  +  $\text{Cr}_2\text{Al}$ ) + Al-rich TiCrAl based alloys also exhibited protective alumina formation at both 1000°C and 800°C.

The Al-lean (37 Al) "single-phase" TiCrAl alloy exhibited nonprotective titania-dominated scale formation at 1000°C and borderline protective alumina scale formation at 800°C. The "single-phase"  $\gamma$  alloy exhibited nonprotective titania-dominated scale formation at both 1000°C and 800°C. Surprisingly, the two-phase  $\gamma$  + TiCrAl alloy, A, exhibited oxidation resistance superior to that of either the "single-phase"  $\gamma$  or "single-phase" Al-lean TiCrAl

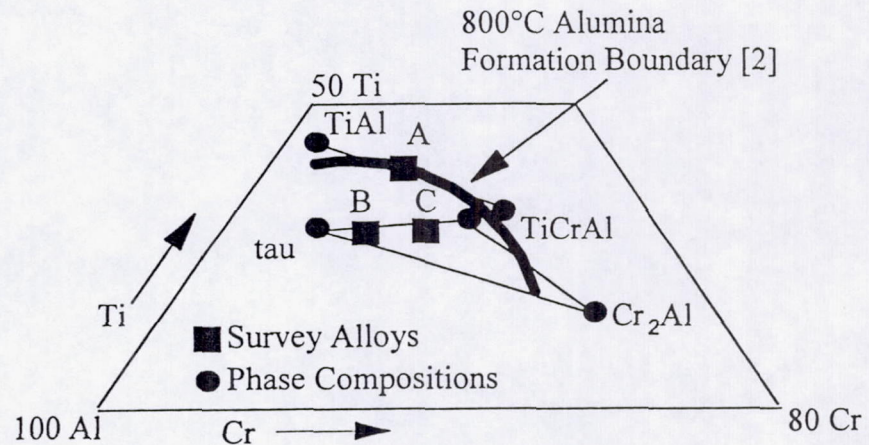


Fig. 1- Schematic of the partial 1000°C isotherm determined from alloys A-C (atom percent) [4].

alloys. A synergistic improvement in oxidation resistance therefore occurred when the  $\gamma$  and TiCrAl phases were combined [8]. The oxidation resistance of alloy A was consistent with borderline protective alumina scale formation. The scale consisted of regions of continuous alumina and isolated regions of titania-based nodules.

A 50Al-35Ti-15Cr alloy was identified as falling on or very near the Al-rich boundary of the  $\gamma$  + TiCrAl two-phase field. This  $\gamma$  + TiCrAl alloy exhibited protective alumina scale formation with no evidence of titania-based nodule formation at both 800°C and 1000°C in air (Fig. 3).

Finally, the weight gains for the TGA exposures in dry air and the box furnace screenings in room air were similar for all alloys except the "single-phase"  $\gamma$  alloy. This alloy exhibited significantly better oxidation resistance in dry air than in room air. It is speculated that this difference is attributable to the humidity of the room air. A mechanistic understanding of this phenomena has not yet been achieved.

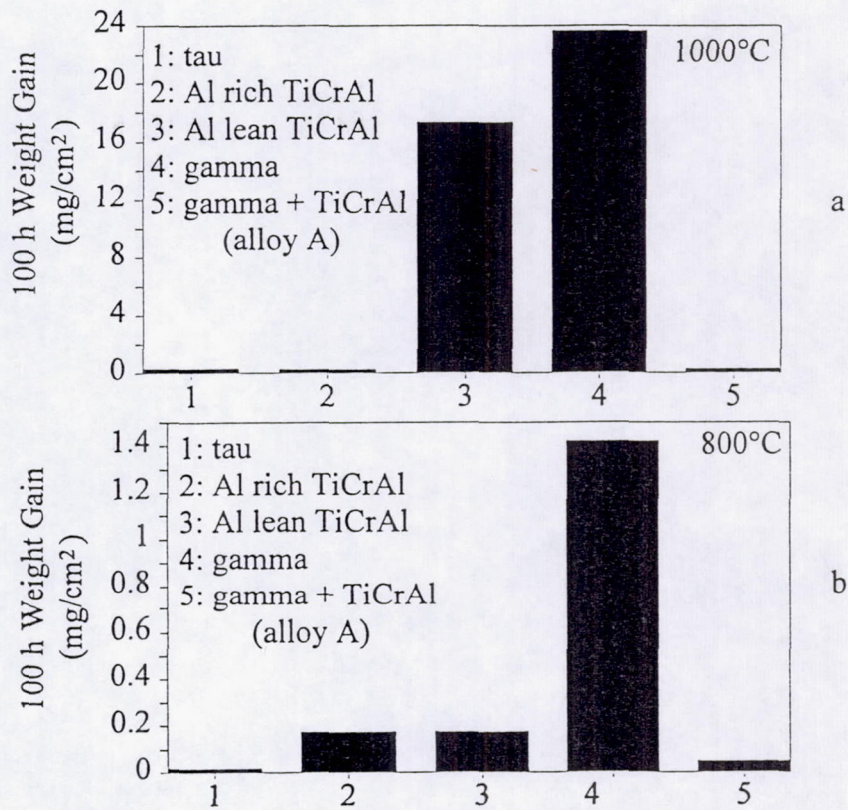


Fig. 2- Isothermal 100 h weight gains in room air. a) 1000°C b) 800°C



Fig. 3- SEM (backscatter mode) cross-section micrograph of 50Al-35Ti-15Cr oxidized for 100 h at 1000°C in air.

## Alloy/Alumina Fiber Reaction Couples

No reaction products were observed (SEM techniques) at the alloy/alumina fiber interface for the "single-phase"  $\gamma$  (Fig 4a),  $\tau$ , or Al-rich TiCrAl alloys. However, the Al-lean TiCrAl "single-phase" alloy reacted with the alumina fiber to form an Al-rich  $\gamma$  layer (identification tentative) at the alloy/alumina interface (Fig 4b).

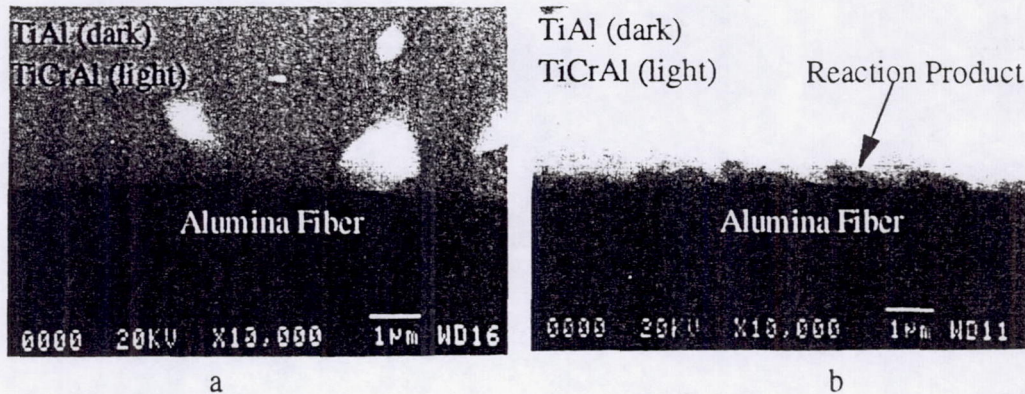


Fig. 4- SEM (backscatter mode) cross-section micrographs of alloy/alumina fiber reaction couples (1000°C / 2 h). a) 52Al-43Ti-5Cr ( $\gamma$  alloy) b) 37Al-34Ti-39Cr (Al-lean TiCrAl alloy)

As noted in the experimental section, all of the "single-phase" alloys contained small amounts of second phases. The "single-phase"  $\gamma$  alloy (52Al-43Ti-5Cr) contained a small volume fraction of the TiCrAl phase and the "single-phase" Al-lean TiCrAl alloy (37Al-34Ti-29Cr) contained a small volume fraction of the  $\gamma$  phase. The compositions of the  $\gamma$  and TiCrAl phases in the  $\gamma$  alloy were 53Al-43Ti-4Cr and 40Al-33Ti-27Cr, respectively. The compositions of the  $\gamma$  and TiCrAl phases in the TiCrAl alloy were 50Al-45Ti-5Cr and 36.5Al-33Ti-30.5Cr, respectively. Therefore, the phases in the  $\gamma$  alloy were slightly Al-rich relative to the phases in the TiCrAl alloy. The reaction of the TiCrAl alloy with the alumina fiber and the apparent stability of the  $\gamma$  alloy therefore suggests that a transition to alumina stability occurs between 50 and 53 Al in  $\gamma$  and 36.5 and 40 Al in TiCrAl.

Stability of a Ti-Al based alloy with alumina is a prerequisite for the formation of a continuous protective alumina layer during oxidation. Alumina is protective by virtue of its extremely low rate of growth. If, in a given alloy, alumina does not possess a stability advantage over Ti-based oxides (which grow at a much faster rate than alumina) then the establishment of a continuous alumina layer will be interrupted by the transient Ti-based oxides and nonprotective oxidation behavior will ensue. The reaction of a Ti-Al based alloy with an alumina fiber in a hot pressed reaction couple experiment does not, however, necessarily indicate that alumina is less thermodynamically stable than Ti based oxides for that alloy.

An oxygen activity gradient will exist between the alloy and the alumina fiber if the alloy does not contain sufficient oxygen for equilibrium with alumina at the outset of the experiment [9]. This gradient can act as the driving force for a reaction between the alloy and the alumina fiber even if alumina is the most stable oxide for the alloy [9]. Recent studies of the

Al-Ti-O system have found that alumina is more stable than Ti-based oxides for Ti-Al alloys with Al contents much less than 50 atom percent [10,11]. Therefore, the transition to alumina stability observed in the present work suggests that the alloy oxygen content needed for equilibrium with alumina decreases sharply between the  $\gamma$  + TiCrAl tie lines defined by the  $\gamma$  and Al-lean TiCrAl alloys, and reaches the point where the nominal oxygen content of the alloy<sup>2</sup> (0.1-0.2 weight percent) is sufficient to stabilize alumina. In other words, the maximum solubility of oxygen in the  $\gamma$  and TiCrAl phases, which must be reached for equilibrium with alumina, decreases significantly between 50 and 53 Al in  $\gamma$  and 36.6 and 40 Al in TiCrAl.

This composition boundary is of engineering importance because significant oxygen dissolution in Ti-based alloys can lead to embrittlement. It may also be of importance for oxidation behavior as well. If the alloy must be saturated with oxygen for alumina stability to be achieved, then the kinetic factors which govern oxygen dissolution into the alloy may negate the thermodynamic stability advantage of alumina over Ti-based oxides. This may prevent the establishment of a continuous alumina layer during the initial stages of oxidation and lead to the formation of rapidly growing, nonprotective Ti based oxides. Such a mechanism could explain the inability of low Al content Al-Ti-Cr alloys to form continuous alumina scales at 800°C in air, where the rate of oxygen dissolution is expected to be low, even though such alloys exhibit continuous alumina scale formation at 1100°C and/or 1300°C in air [2]. More detailed studies and duplicate tests of alloy/alumina reaction couples are needed to support this conjecture.

### Microhardness

Microhardness data for the  $\tau$ , TiCrAl laves, and  $\gamma$  phases (averaged from alloys A-C and the "single-phase" alloys) are shown in Fig. 5. Both the Al-rich and the Al-lean TiCrAl laves phases had VHN's of over 700 and microcracks were observed emanating from the microhardness

indentations. The formation of microcracks using an indent load of only 100 g is indicative of extreme brittleness. The  $\tau$  phase had a VHN of 315. However, the decomposition of the  $\tau$  phase to  $Al_2Ti$  and  $Cr_2Al$  after exposure at 800°C resulted in a 160 % increase in the VHN to 515. Both the  $Al_2Ti$  and  $Cr_2Al$  phases are brittle [6]. The  $\gamma$  phase had a VHN of  $\approx 350$  after both the 1000°C and 800°C exposures and plastic deformation markings were observed near the microhardness indentations. Single-phase  $\gamma$  alloys exhibit room temperature plastic fracture strains in the 0.5%-1.0% range [12]. Therefore, the only option for even limited ductility in the protective alumina-forming composition range of the Al-Ti-Cr system is an alloy based on the  $\gamma$  phase.

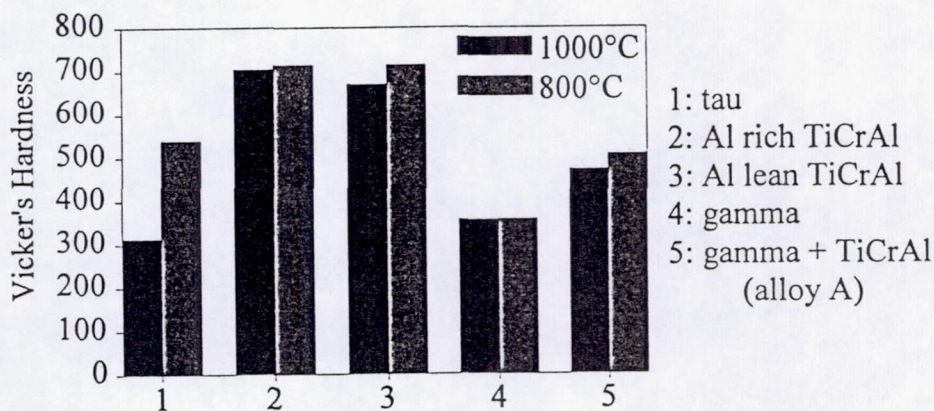


Fig. 5- Vickers microhardness data (100 g, 15 s) for alloys heat treated for 100 h at 1000°C or 800°C.

## SUMMARY AND CONCLUSIONS

Two-phase  $\gamma + \text{TiCrAl}$  Al-Ti-Cr alloys offer the potential for protective alumina scale formation and limited room temperature ductility. The  $\gamma$  phase is the only nonbrittle phase in the alumina-forming Al-Ti-Cr composition range identified by Meier et al.. However, protective alumina scale formation is not observed unless the microstructure also contains the TiCrAl laves phase, which is brittle. The composition range of interest is defined at low Al concentrations by the  $\gamma/\text{TiCrAl}$  tie line of 37Al-34Ti-29Cr (the Al-lean TiCrAl alloy), which was not stable with alumina at nominal alloy oxygen concentrations. The upper Al limit is defined by the  $\gamma/\text{TiCrAl}$  tie-line of the alloy 50Al-35Ti-15Cr, which is located on or near the Al-rich extent of the  $\gamma + \text{TiCrAl}$  two-phase field. Future work will concentrate on optimizing ductility by 1) selecting alloy compositions in which the  $\gamma$  phase is continuous in order to disrupt the connectivity of the brittle TiCrAl phase and 2) by lowering the Al content in the  $\gamma$  phase. Preliminary results indicate that  $\gamma$ -continuous  $\gamma + \text{TiCrAl}$  alloys are capable of protective alumina scale formation [13].

## ACKNOWLEDGEMENTS

The authors wish to thank A.K. Misra of NYMA, Inc. for his significant input into the design and interpretation of the alloy/alumina reaction couple experiments. One author (MPB) also wishes to acknowledge the financial support of a National Research Council Post-Doctoral Research Associateship. This research was funded under the NASA HITEMP program.

## REFERENCES

1. G.H. Meier, R.A. Perkins, J.C. Schaeffer, and R. L. McCarron, GE Aircraft Engines Interim Report No. 1, Naval Air Development Center Contract N62269-90-C-0287 (March 1991).
2. R.A. Perkins and G.H. Meier, in Proceedings of the Industry-University Advanced Materials Conference II, Smith, F. ed., Advanced Materials Institute, p. 92 (1989).
3. D.W. McKee and S.C. Huang, Cor. Sci., 33, p. 1899 (1992).
4. M.P. Brady, J.L. Smialek, and F. Terepka, submitted to Scripta Met. (Sept. 1994).
5. M.P. Brady, J.L. Smialek, and D.L. Humphrey, NASA Lewis 1994 HITEMP Review, 2, pp. 45-1 to 45-11 (1994).
6. J.L. Klansky, J.P. Nic, and D.E. Mikkola, J. Mater. Res., 9, p. 255 (1994).
7. G.H. Meier, N. Birks, F.S. Pettit, R.A. Perkins, and H.J. Grabke, in Structural Intermetallics, R. Darolia, J.J. Lewandowski, C.T. Liu, P.L. Martin, D.B. Miracle, and M.V. Nathal, TMS, Warrendale, PA, p. 869 (1993).
8. M.P. Brady, J.L. Smialek, and D.L. Humphrey, Electrochemical Society Extended Abstracts, Fall (1994).
9. B. Gleeson, private communication (Oct. 1994).
10. Y. Chen, D.J. Young, and B. Gleeson, Materials Letters (in press).
11. M.-X Zhang, K.-C Hsieh, J. DeKock, and Y.A. Chang, Scripta Met., 27, pp. 1361-1366 (1992).
12. S-C. Huang and E.L. Hall, Met. Trans. A, 22, 1991, p. 2619.
13. M.P. Brady and J.L. Smialek, to be published in Nasa Lewis Research and Technology (1994).